Progress in Pediatric Cardiology 53 (2019) 28–36

Contents lists available at ScienceDirect

Progress in Pediatric Cardiology

journal homepage: www.elsevier.com/locate/ppedcard

Real-time transthoracic vector flow imaging of the heart in pediatric patients☆

R. Thomas Collins II[a,*], Megan E. Laughlin[b], Sean M. Lang[c], Elijah H. Bolin[d,e], Joshua A. Daily[d,e], Hanna A. Jensen[b], Morten O. Jensen[b]

[a] Stanford University, Department of Pediatrics, 750 Welch Road, Palo Alto, CA 94304, United States
[b] University of Arkansas, Department of Biomedical Engineering, 790 W. Dickson St., Fayetteville, AR 72701, United States
[c] Cincinnati Children's Hospital Medical Center, Department of Cardiology, 3333 Burnet Ave., Cincinnati, OH 45229, United States
[d] University of Arkansas for Medical Sciences, Department of Pediatrics, 1 Children's Way, Little Rock, AR 72202, United States
[e] Arkansas Children's Research Institute, 1 Children's Way, Little Rock, AR 72202, United States

ARTICLE INFO

Keywords:
Transthoracic echocardiography
Congenital heart disease
Velocity flow
Vector flow imaging

ABSTRACT

In children with congenital heart defects, Doppler ultrasound is the standard, bedside imaging modality. However, precise characterization of blood flow is challenging due to angle-dependent and one-dimensional velocity estimation. Contrast agent free Vector Flow Imaging is a new ultrasound technology that enables angle-independent visualization of the detailed flow field. Two piglets, one with normal cardiac anatomy and one with congenital heart disease comprised of valvular pulmonary stenosis, a dilated main pulmonary artery, and an incomplete atrioventricular canal defect, were imaged transthoracically and epicardially using a BK Ultrasound bk5000 with built-in vector flow imaging and a 5 MHz linear probe. Subsequently, two children, one with normal cardiac anatomy and one with congenital heart disease comprised of aortic valve stenosis and coarctation of the aorta were imaged transthoracically. Transthoracic two-dimensional echocardiography and vector flow imaging were readily performed in both animals and were limited only by the geometry of the porcine thorax. In addition, transthoracic vector flow imaging was successfully performed in both children, and abnormal flow secondary to cardiac anomalies was visible. Adequate penetration was obtained to a depth of 6.5 cm. Our group has previously demonstrated for the first time that transthoracic vector flow imaging echocardiography is feasible and practicable in pediatric-sized patients, and this paper describes examples of these concepts and in-depth comparisons with traditional imaging modalities. This paper demonstrates that commercially available vector flow imaging technology can be utilized in pediatric cardiac applications as a bedside transthoracic imaging modality, providing advanced detail of blood flow patterns within the cardiac chambers, across valves, and in the great arteries.

1. Introduction

Congenital heart disease occurs in about 1% of live births when bicuspid aortic valve is excluded [1]. Echocardiography is the primary modality for the initial evaluation and long-term follow-up of children with congenital heart disease. Doppler ultrasound provides key information about cardiac valve function, as well as characterization of intracardiac shunts. However, the accurate estimation of intracardiac velocities and pressure differences is dependent on the angle of insonation. Oftentimes, the anatomy of a patient's chest wall or the geometry of a malformed heart precludes an appropriate angle of interrogation [2].

Cardiac magnetic resonance imaging can provide angle-independent assessment of blood flow. Recently, four-dimensional magnetic resonance imaging techniques have allowed for advanced assessment of complex flow dynamics [3]. However, cardiac magnetic resonance imaging, and four-dimensional flow in particular, requires immobile and expensive equipment, along with a cadre of specialized personnel. In addition, magnetic resonance imaging often requires anesthesia, particularly in young children. A non-invasive, angle-independent, ultrasound-based imaging modality that provides advanced hemodynamic flow assessment along with bedside availability and

☆ This work was first presented at the 50th Annual Meeting of the Biomedical Engineering Society on October 18th, 2018.

* Corresponding author at: 750 Welch Road Suite 321, Palo Alto, CA 94304, United States.
E-mail addresses: tomcollins@stanford.edu (R.T. Collins II), mew037@uark.edu (M.E. Laughlin), sean.lang@cchmc.org (S.M. Lang), EHBolin@uams.edu (E.H. Bolin), JADaily@uams.edu (J.A. Daily), hkjensen@uark.edu (H.A. Jensen), mojensen@uark.edu (M.O. Jensen).

https://doi.org/10.1016/j.ppedcard.2019.02.003
Received 26 July 2018; Received in revised form 17 January 2019; Accepted 21 February 2019
Available online 05 March 2019

mobility would be ideal for the evaluation of children with congenital heart disease.

Vector flow imaging is a recently developed, ultrasound-based imaging method that provides real-time, angle-independent visualization of flow. Vector flow imaging uses transverse oscillation to assess both transverse and axial velocity components simultaneously via dual-peaked receiver apodization, an optical filtering technique, that creates a double-oscillating field sensitive to full vector motion in the imaging plane [4,5]. The penetration depth of commercially available vector flow imaging transducers has been previously estimated to be 5 cm, and thus most prior studies have been limited to epicardial use [6]. The use of vector flow imaging in pediatric patients and pediatric animal models have preliminarily been described by our group and others, and we hypothesize that the use of a commercially available vector flow imaging ultrasound system could be used to perform transthoracic echocardiography in a pediatric-sized animal model as well as in pediatric patients with congenital heart disease [7,8]. The aim was to demonstrate the feasibility of transthoracic cardiac imaging with a commercially available vector flow imaging system and provide a detailed comparison with existing, traditional pediatric cardiac imaging modalities.

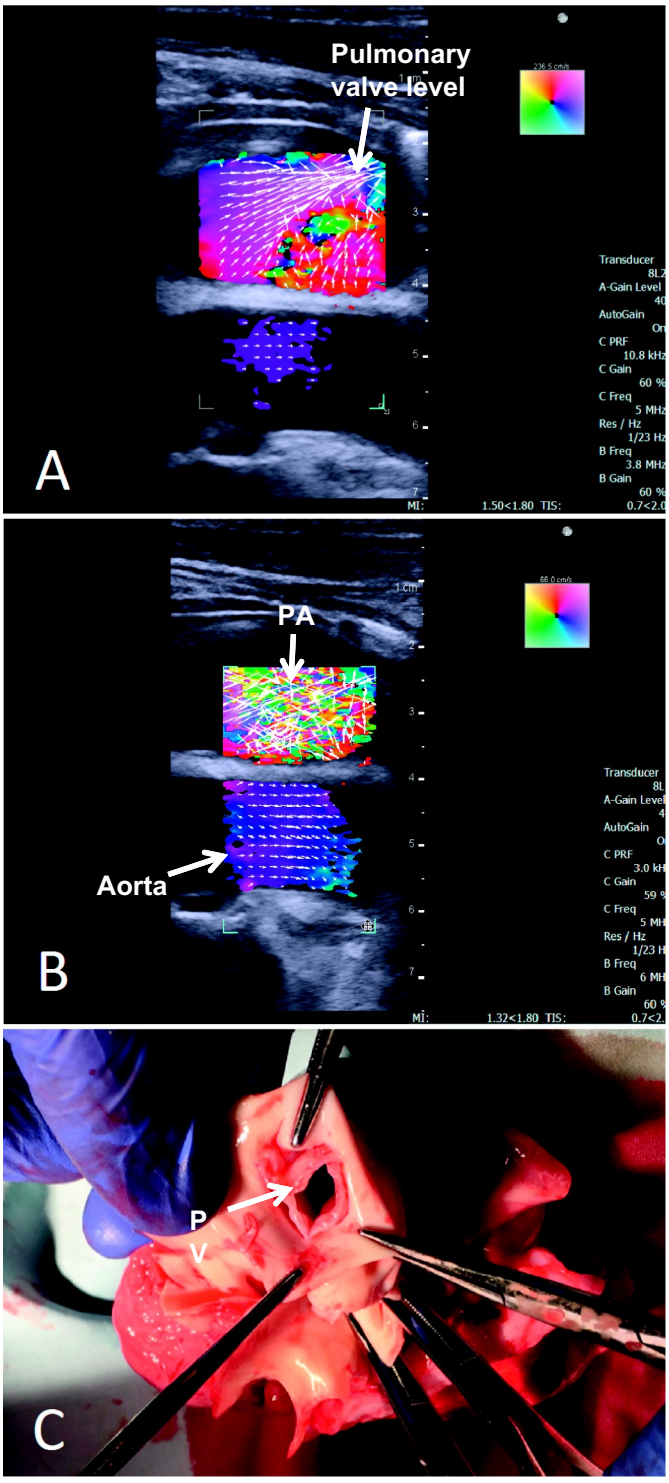

Fig. 1. Panel A: Parasternal long-axis image with vector flow imaging in Animal 2 demonstrates flow acceleration and narrowing of the blood column as it moves anteriorly through the stenotic pulmonary valve (PV). Flow is demonstrated swirling in behind the pulmonary valve on the distal side of the valve. Panel B: Markedly turbulent flow is demonstrated in the anterior pulmonary artery (PA) above the level of the pulmonary valve. Flow in the aorta (posterior) is laminar and low velocity. Panel C: The explanted heart from Animal 2 demonstrating thickened, nodular pulmonary valve cusps. Note: The square color legend on the top-right corner of each screenshot indicates direction and magnitude of flow at each colored pixel in the images. Each white arrow represents a dataset containing velocity and directional data. The spatial concentration of these arrows can be increased or decreased to aid the visual assessment of the flow field, in combination with the color coding scheme. As flow velocity increases, the arrows lengthen. In the presence of turbulent flow, the vector flow imaging arrows are not aligned and are disarrayed. (For interpretation of the references to color in this figure legend, the reader is referred to the web version of this article.)

2. Methods

2.1. Animal protocol

The study was approved by the University of Arkansas for Medical Sciences Institutional Animal Care and Use Committee. Two juvenile pigs were obtained from a commercial farm (Metz Farms, Russellville, AR). To assess the ability to perform transthoracic vector flow imaging in different patient sizes, a 4.5 kg piglet (Animal 1) was used to model imaging in an infant, and a 22 kg piglet (Animal 2) was used to model imaging in a school-aged child.

The piglets were anesthetized and then studied using a BK Ultrasound bk5000 system with built-in vector flow imaging (BK Medical, Peabody, MA) equipped with a 5 MHz linear probe (Linear Array 8 L2, BK Medical) to perform transthoracic and epicardial echocardiography. Transthoracic imaging was performed sequentially from subcostal, apical, and parasternal views. All scan settings, such as pulse repetition frequency, frequency, and thus velocity range, were optimized for each subject, as seen on all videos. Multiple transthoracic images were acquired at the level of the atrial septum, atrioventricular valves, and semilunar valves, as well as within the ventricles and great arteries, using both standard two-dimensional and vector flow imaging. Thereafter, a standard median sternotomy was performed, and epicardial images were obtained. Following the imaging protocol, euthanasia was performed, and both hearts were explanted for pathologic examination and confirmation of imaging findings. All animals received humane care and the appropriate institutional guidelines were followed throughout the study.

2.2. Clinical protocol

The University of Arkansas for Medical Sciences Institutional Review Board separately approved the human portion of the study and thus the protocol conformed to all ethical guidelines. All patient

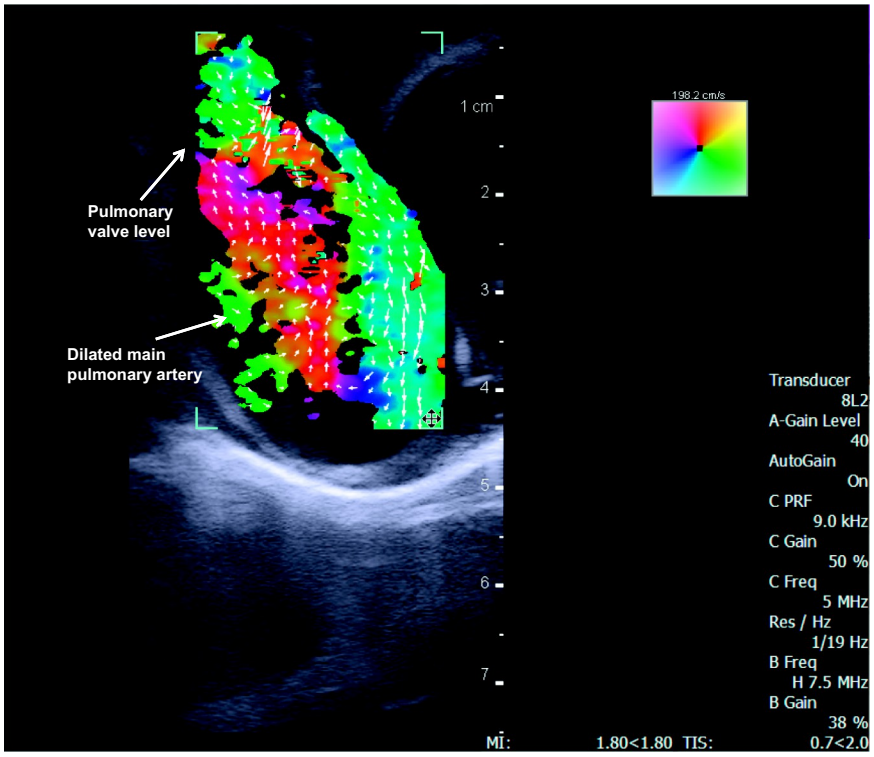

Fig. 2. Parasternal imaging of the main pulmonary artery (PA) with vector flow imaging in Animal 2 demonstrating swirling of flow within the dilated main pulmonary artery.

information was de-identified and stored in a secured location. Informed consent was obtained for all participating patients. Two potential subjects were identified and scanned, both three months of age with one being 6.4 kg (Patient 1) and the other 6.8 kg (Patient 2). One had a structurally normal heart (Patient 1), and the other exhibited valvular aortic stenosis and coarctation of the aorta (Patient 2). The same BK Medical bk5000 system with vector flow imaging and 5 MHz linear probe was used as in the animal study. Again, all scan settings were optimized for each patient. Transthoracic images were obtained from the parasternal long-axis and short-axis views. The study images for Patient 1 were obtained without sedation, and those for Patient 2 were obtained under anesthesia both before and after transcatheter balloon aortic valvuloplasty and balloon angioplasty of the site of coarctation.

3. Results

Both pigs had mesocardia. Animal 1 was found to have a structurally normal heart (Video 1-3). Animal 2 was serendipitously found to have congenital heart disease comprised of valvular pulmonary stenosis (Fig. 1; Videos 4 & 5), a dilated main pulmonary artery (Fig. 2; Video 6), and an incomplete atrioventricular canal defect (Fig. 3; Video 7). Transthoracic two-dimensional echocardiography and vector flow imaging were readily performed in both animals and were limited only by the geometry of the porcine thorax. Adequate penetration was obtained to a depth of 6.5 cm (maximum depths were 5 cm (Animal 1, 4.5 kg), 6 cm (Animal 2, 22 kg), 6 cm (Patient 2, 6.4 kg), and 6.5 cm (Patient 2, 6.8 kg)). No apparent differences in quality were observed between the 2D echocardiography and vector flow imaging images, only the fact that vector flow imaging provided more visually detailed flow information.

Fig. 4 compares transthoracic and epicardial images acquired in both animals. A qualitative assessment of the difference in obtaining diagnostic parameters between color-Doppler, echocardiographic particle imaging velocimetry, vector flow imaging, and phase-encoded magnetic resonance imaging during examination is listed in Table 1 (adapted from Sengupta et al. [9]).

The normal cardiac anatomy of Patient 1 was confirmed, and structures were readily identifiable (Fig. 5; Video 8). Patient 2 was successfully imaged both before (Fig. 6A; Video 9) and after aortic valvuloplasty and angioplasty of coarctation (Fig. 6B; Video 10). Significantly turbulent flow was observed across the stenotic aortic valve and continuing into the ascending aorta, as well as at the site of the coarctation of the aorta. Following the procedure, the turbulent flow was improved, though flow was not normal and laminar (Fig. 6). Sufficient images were obtained from Patient 1, who received no anesthesia and anesthetized Patient 2. Adequate penetration was obtained to a depth of 6.5 cm.

4. Discussion

We have demonstrated for the first time that transthoracic echocardiography with vector flow imaging is feasible and practicable in a pediatric-sized animal model and in pediatric patients using a commercially available system [7]. The quality of vector flow imaging data was equivalent between transthoracic and epicardial images, and between pig and human images. Additionally, vector flow imaging was feasible both with and without patient anesthetization. Adequate

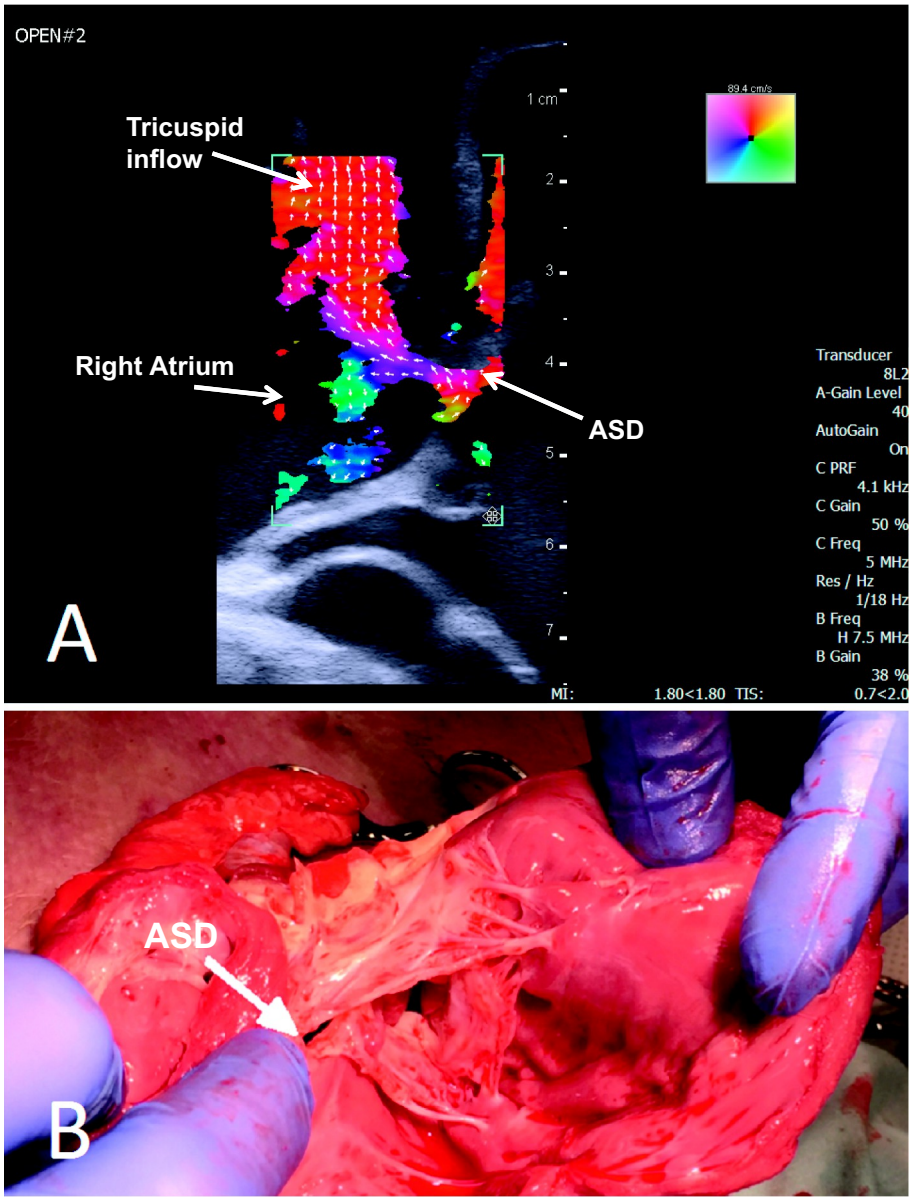

Fig. 3. Panel A: Apical imaging of the atrial septum and tricuspid valve inflow with vector flow imaging in Animal 2 demonstrates flow passing across an atrial septal defect. Panel B: The explanted heart from Animal 2 demonstrating a cleft in the anterior leaflet of the left atrioventricular valve with the valve tissue passing through an atrial septal defect (white arrow).

penetration was obtained to a depth of 6.5 cm in human patients while being able to readily identify all cardiac structures and observe flow throughout the heart. These findings demonstrate the feasibility of transthoracic vector flow image and suggest that it can be employed in the assessment of pediatric congenital heart disease. The lack of anesthetization required for imaging offers an additional advantage of vector flow imaging as a bedside imaging modality, especially since patients with complex conditions exhibiting cardiac anomalies, such as Williams syndrome, have a heightened risk of adverse effects to anesthesia [10]. Additionally, vector flow imaging may offer additional benefits in providing an improved definition of the nature of stenosis and a more detailed assessment of flow derangement with systolic or diastolic dysfunction. As this was a feasibility study, no quantification was performed; however, our results align with those of Brandt et al. in that the transthoracic 2D echocardiography images had similar quality to that of the transthoracic vector flow imaging images in the animal subjects [11,12]. Future studies will focus on quantification using the vector information provided by vector flow imaging, which will require the development of new software for this novel application.

Vector flow imaging represents the sum of traditionally used Doppler ultrasound modalities with the additional benefit of determination of flow directionality through obtaining new insonation windows to cardiac flow [12]. Given the complex flow dynamics often seen in patients with congenital heart disease, the ability to determine

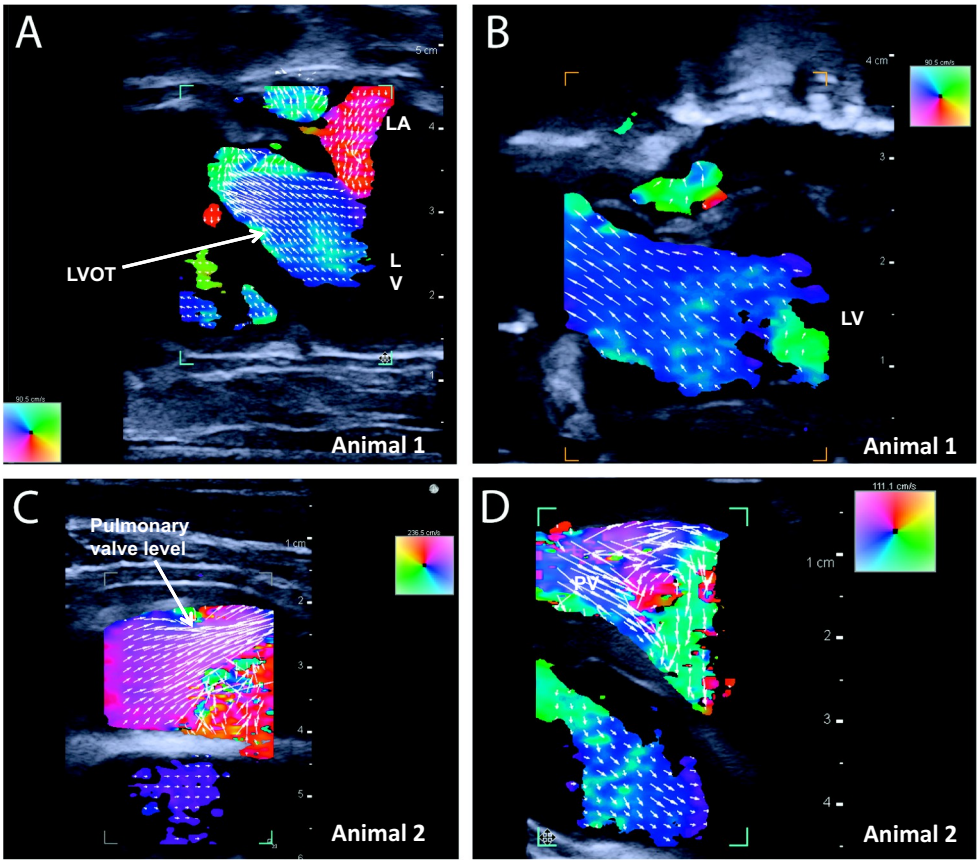

Fig. 4. Panel A. Transthoracic vector flow imaging in Animal 1 demonstrates organized, pseudo laminar flow from the left ventricle (LV) out the left ventricular outflow tract (LVOT). Notably, as the flow accelerates slightly in the left ventricular outflow tract, the vector flow imaging arrows are more elongated than those within the left ventricular cavity. Additionally, in the far-field, flow is demonstrated into the left atrium (LA). Panel B. Epicardial vector flow imaging in Animal 1 demonstrates flow from the left ventricle out the left ventricular outflow tract that is similar to those from transthoracic imaging. Of note, the resolution of the epicardial image is less than that on transthoracic imaging. Panel C. Transthoracic vector flow imaging in Animal 2 demonstrates flow across the anteriorly located stenotic pulmonary valve. The vector flow imaging demonstrates flow acceleration and narrowing of the blood column as it passes anteriorly across the stenotic pulmonary valve. The vector flow imaging arrows lengthen as the flow accelerates toward and crosses the pulmonary valve. Flow is demonstrated swirling in behind the pulmonary valve. Additionally, in the far-field, laminar flow is demonstrated in the aorta. Panel D. Epicardial vector flow imaging in Animal 2 demonstrates accelerated flow with a narrowed blood column across the stenotic pulmonary valve similar to that seen from transthoracic imaging. Again, laminar flow is demonstrated in the aorta.

cardiovascular fluid dynamics more accurately is of particular interest. The use of four-dimensional flow analysis via magnetic resonance imaging for such a purpose is attractive, but is limited by several factors such as availability, need for specialized training, and sedation in pediatric patients [3]. An ultrasound-based modality such as vector flow imaging is ideal for hemodynamic flow assessments in pediatric patients.

Vector flow imaging performed intraoperatively has been used to quantify flow complexity using methods such as vector concentration which has exhibited a strong correlation to degree of stenosis [13]. Additionally, vector flow imaging has been used for pressure gradient estimations at the carotid bifurcation and at the aortic valve, along with vorticity estimations in the ascending aorta and carotid bulb [14–16]. The study of vortex formation in the cardiac chambers has also been demonstrated with vector flow mapping and vector flow imaging [17]. Although not yet available commercially, vector flow imaging has also been extended to three-dimensional use on an experimental scanner to assess flow in the common carotid artery and quantification of arterial volumetric flow rate, further extending its potential applications and benefits beyond that of MRI and standard echocardiography systems [18,19].

While vector flow imaging is novel and promises great opportunity for improving the non-invasive assessment of cardiovascular hemodynamics, particle image velocimetry is a commercially available alternative to vector flow imaging. Particle image velocimetry relies on tracking particles in the flow field in a manner similar to speckle tracking [20]. The penetration depth of echocardiographic particle image velocimetry is better than vector flow imaging, which may be of benefit in adult-sized patients, but is less important in pediatric patients. However, certain echocardiographic particle image velocimetry systems are limited by the need for contrast agents [21,22]. Additionally, echocardiographic particle image velocimetry does not provide instantaneous velocities, whereas vector flow imaging, similarly to regular color Doppler, derives the velocity from the frequency shift of one echo from a particle that is moving and does not attempt to "visually" track a particle between two successive frames. Hence, echocardiographic particle image velocimetry relies on the spatial resolution of the echocardiography images, and is more error-prone than true vector velocity signal when operating within the penetration depth limitations of the vector flow imaging technology. Furthermore, the spatial resolution of standard echocardiography has not been sufficient for echocardiographic particle image velocimetry to be clinically useful [20,23].

Ultrasound-based vector flow imaging has thus far been utilized primarily for the assessment of relatively superficial structures including the carotid artery [24], arteriovenous fistulae for hemodialysis [25], and the femoral vein [26]. The use of vector flow imaging in the assessment of cardiac structures has previously been limited to epicardial imaging [5]. We demonstrate that transthoracic vector flow imaging has sufficient penetration and visualization for pediatric clinical applications. Future work will focus on quantifications using vector flow imaging, of particular interest being vortex assessment in the left

Table 1
Comparing vector flow imaging with other flow diagnostic techniques.
(Adapted from Sengupta et al. [9])

	Echocardiography			MRI
	Color-Doppler	Echo-PIV	Vector flow imaging	Phase-encoded MRI
Assessment of flow directionality in 3 dimensions	Limited to assessment of flow along the line of insonation	Good assessment of 2 dimensions in-plane; no through-plane assessment	Excellent assessment of in-plane flow; no through-plane assessment	Good assessment of directionality of flow in all directions
Spatial resolution	Excellent 2D spatial resolution; Acceptable 3D spatial resolution	Good 2D spatial resolution	Good 2D spatial resolution (voxel size $< 1\,m^{-3}$)	Good spatial resolution in all directions
Frame rate	Excellent 2D temporal resolution (> 50 fps), acceptable in 3D	High temporal resolution of velocity fields when acquisition is over multiple cardiac cycles	High temporal resolution of velocity fields (> 30 fps) during a single cardiac cycle	Good temporal resolution (25 fps) derived from phases calculated over many cardiac cycles
Low-velocity accuracy	Possibly underestimated and/or noise sensitive	Excellent visualization with high accuracy	Excellent visualization with high accuracy	Low velocities are inaccurate if high velocities are also present
High-velocity accuracy	Highly accurate within Nyquist limits	Possibly underestimated	Accurate (< 10%)	Accurate up to the chosen velocity-encoded limit; inaccurate if the stream width is less than a voxel
Scan time	Fast, real-time visualization	Image acquisition is over multiple cardiac cycles; off-line analysis is required	Fast, real-time visualization	Long scan times (10–20 min) for acquisition of a 3D dataset
Breath-holding requirement	No breath-holding requirements	Improved imaging with breath-hold, but it is not necessary	No breath-holding requirements	Used for short, unidirectional velocity acquisitions
Impact of implanted devices	Typically inconsequential	Typically inconsequential	Typically inconsequential	Image artifacts from metals in stents, valve rings, etc.; MRI is ruled out in most pacemakers and all AICDs
Applications	Flow visualization throughout the heart and great vessels	Flow visualization throughout the heart and great vessels	Flow visualization throughout the heart and great vessels; assessment of volume flow within the great arteries	Flow visualization and measurement of volume flow through all cardiac chambers and large vessels

PIV = particle imaging velocimetry, MRI = magnetic resonance imaging, 2D = two-dimensional, 3D = three-dimensional, FPS = frames per second, AICD = automatic implantable cardioverter-defibrillator.

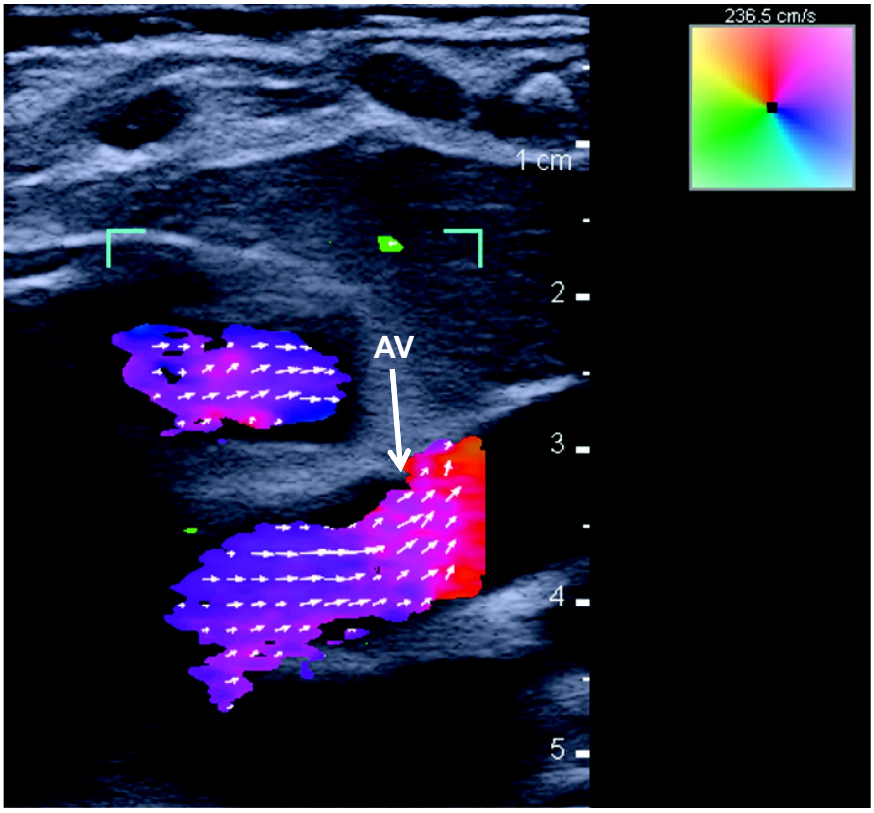

Fig. 5. Transthoracic vector flow imaging vector flow imaging in Patient 1 demonstrates a healthy anatomy with laminar flow across the aortic valve. No turbulence is observed. AV indicates aortic valve.

ventricle as irregular vorticity formation is believed to lead to irreversible left ventricular remodeling in children [27].

5. Limitations

This study has several limitations. The ultrasound probe was not designed specifically for cardiac assessment, and one is not currently available. Although the image quality is currently very good, a probe optimized for cardiac imaging would likely be superior. Also, because this was a proof of concept study to demonstrate that vector flow imaging can be obtained in pediatric patients, we did not attempt to measure angle-independent maximal velocities and pressure differences. Additionally, the inclusion of only two human patients who were both infants may limit the generalizability to a broader pediatric population as older, larger children are likely more difficult to image.

6. Conclusions

We demonstrated that vector flow imaging via transthoracic windows was possible in both an animal and a child with congenital heart disease. Vector flow imaging is a novel tool that holds the promise of being able to quantify hemodynamics in ways heretofore not readily available. Studies with larger cohorts are currently underway to determine the ability of vector flow imaging to assess flow characteristics in both healthy and diseased hearts in a broad range of infants and children.

Supplementary data to this article can be found online at https://doi.org/10.1016/j.ppedcard.2019.02.003.

Declarations of interest

None.

Conflicts of interest

None. Authors declare there are no significant competing financial, professional, or personal interests that might have influenced the performance or presentation of the work described in this manuscript.

Statement of ethical treatment of animals

The study was approved by the University of Arkansas for Medical Sciences Institutional Animal Care and Use Committee.

Funding source

This project was supported by the Arkansas Children's Research Institute, the Collaborative Nutrition Pilot Grant, and the Arkansas Research Alliance.

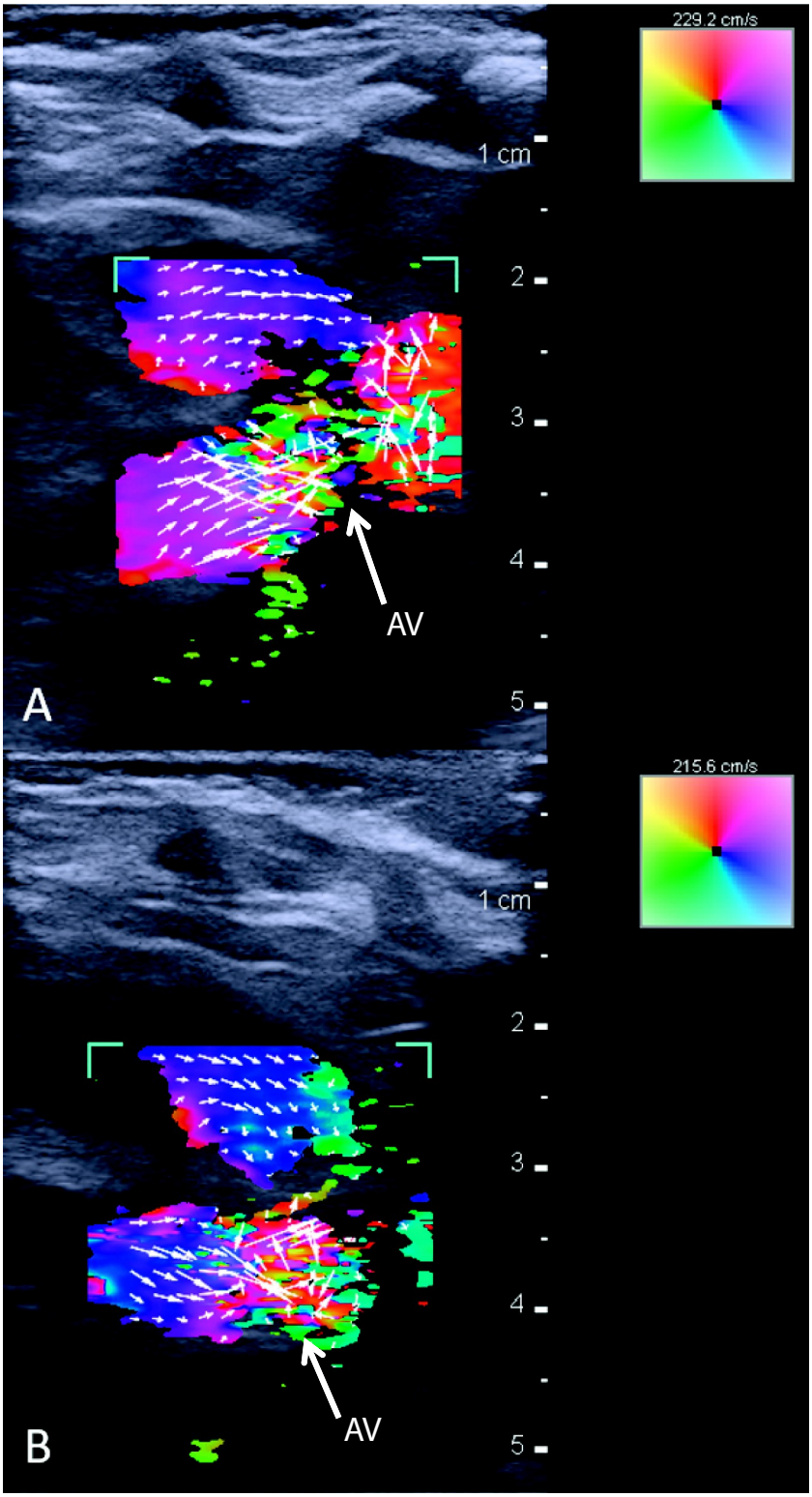

Fig. 6. Panel A. Parasternal transthoracic imaging of the aortic valve (AV) is performed on Patient 2 using vector flow imaging vector flow imaging before procedures. Stenosis at the level of the AV can be observed, as indicated by heavily turbulent flow with high and disorganized velocities across the narrow valve. Panel B. Parasternal transthoracic imaging of the AV is again performed using vector flow imaging following balloon valvuloplasty of the AV and balloon angioplasty of the stenotic valve. A decrease in turbulence is observed following the procedures and the velocities are lowered; however, turbulence is still present.

References

[1] Hoffman JI, Kaplan S. The incidence of congenital heart disease. J Am Coll Cardiol 2002;39(12):1890–900.
[2] Braverman AC, Guven H, Beardslee MA, Makan M, Kates AM, Moon MR. The bicuspid aortic valve. Curr Probl Cardiol 2005;30(9):470–522.
[3] Markl M, Schnell S, Wu C, Bollache E, Jarvis K, Barker AJ, et al. Advanced flow MRI: emerging techniques and applications. Clin Radiol 2016;71(8):779–95.
[4] Tysoe C, Evans DH. Bias in mean frequency estimation of Doppler signals due to wall clutter filters. Ultrasound Med Biol 1995;21(5):671–7.
[5] Jensen JA, Munk P. A new method for estimation of velocity vectors. IEEE Trans Ultrason

Ferroelect Freq Control 1998;45:837–51.
[6] Hansen KL, Moller-Sorensen H, Pedersen MM, Hansen PM, Kjaergaard J, Lund JT, et al. First report on intraoperative vector flow imaging of the heart among patients with healthy and diseased aortic valves. Ultrasonics. 2015;56:243–50.
[7] Collins IIRT, Laughlin M, Jensen H, Lang S, Bolin E, Daily J, et al. Vector flow imaging for cardiovascular applications in pediatric patients and models. Presented at the 2018 Biomedical Engineering Society annual conference, Atlanta, Georgia, Oct. 18th. 2018.
[8] Hansen KL, Juul K, Møller-Sørensen H, Nilsson JC, Jensen JA, Nielsen MB. Pediatric transthoracic cardiac vector flow imaging - a preliminary pictorial study. Ultrasound Int Open 2019;5:E20–6.
[9] Sengupta PP, Pedrizzetti G, Kilner PJ, Kheradvar A, Ebbers T, Tonti G, et al. Emerging trends in CV flow visualization. JACC Cardiovasc Imaging 2012;5(3):305–16.
[10] Collins II RT. Cardiovascular disease in Williams syndrome. Circulation 2013;127:2125–34.
[11] Brandt AH, Hansen KL, Ewertsen C, Holbek S, Olesen JB, Moshavegh, et al. A comparison study of vector velocity, spectral doppler, and magnetic resonance of blood flow in the common carotid artery. Ultrasound Med Biol 2018;44(8):1751–61.
[12] Brandt AH, Moshavegh R, Hansen KL, Bechsgaard T, Lönn L, Jensen JA, et al. Vector flow imaging compared with pulse wave Doppler for estimation of peak velocity in the portal vein. Ultrasound Med Biol 2018;44(3):593–601.
[13] Hansen KL, Møller-Sørensen Kjaergaard J, Jensen MB, Lund JT, Pedersen MM, et al. Intra-operative vector flow imaging using ultrasound of the ascending aorta among 40 patients with normal, stenotic and replaced aortic valves. Ultrasound Med Biol 2016;42(10):2414–22.
[14] Olesen JB, Villagómez-Hoyos CA, Møller ND, Ewertsen C, Hansen KL, Nielsen MB, et al. Noninvasive estimation of pressure changes using 2-D vector velocity ultrasound: an experimental study with in vivo examples. IEEE Trans Ultrason Ferroelectr Freq Control 2018;65(5):709–19.
[15] Hansen KL, Møller-Sørensen H, Kjaergaard J, Jensen MB, Jensen JA, Nielsen MB. Aortic valve stenosis increases helical flow and flow complexity: a study of intra-operative cardiac vector flow imaging. Ultrasound Med Biol 2017;43(8):1607–17.
[16] Chen Z, Li Y, Li C, Tang H, Wang H, Zhong Y, et al. Right ventricular dissipative energy loss detected by vector flow mapping in children: characteristics of normal values. J Ultrasound Med 2019;38(1):131–40.
[17] Goddi A, Bortolotto C, Raciti MV, Fiorina I, Aiani L, Magistretti G, et al. High-frame rate vector flow imaging of the carotid bifurcation in healthy adults: a comparison with color Doppler imaging. J Ultrasound Med 2018;37(9):2263–75.
[18] Holbek S, Hansen KL, Bouzari H, Ewertsen C, Stuart MB, Thomsen C, et al. Common carotid artery flow measured by 3-D ultrasonic vector flow imaging and validated with magnetic resonance imaging. Ultrasound Med Biol 2017;43(10):2213–20.
[19] Correia M, Provost J, Tanter M, Pernot M. 4D ultrafast ultrasound flow imaging: in vivo quantification of arterial volumetric flow rate in a single heartbeat. Phys Med Biol 2016;61(23):L48–61.
[20] Kheradvar A, Houle H, Pedrizzetti G, Tonti G, Belcik T, Ashraf M, et al. Echocardiographic particle image velocimetry: a novel technique for quantification of left ventricular blood vorticity pattern. J Am Soc Echocardiogr 2010;23(1):86–94.
[21] Kim HB, Hertzberg JR, Shandas R. Development and validation of echo PIV. Experiments in Fluids 2004;36(3):455–62.
[22] Westerdale J, Belohlavek M, McMahon EM, Jiamsripong P, Heys JJ, Milano M. Flow velocity vector fields by ultrasound particle imaging velocimetry: in vitro comparison with optical flow velocimetry. J Ultrasound Med 2011;30(2):187–95.
[23] Falahatpisheh A, Rickers C, Gabbert D, Heng EL, Stalder A, Kramer HH, et al. Simplified Bernoulli's method significantly underestimates pulmonary transvalvular pressure drop. J Magn Reson Imaging 2016;43(6):1313–9.
[24] Udesen J, Nielsen MB, Nielsen KR, Jensen JA. Examples of in vivo blood vector velocity estimation. Ultrasound Med Biol 2007;33(4):541–8.
[25] Hansen PM, Olesen JB, Pihl MJ, Lange T, Heerwagen S, Pedersen MM, et al. Volume flow in arteriovenous fistulas using vector velocity ultrasound. Ultrasound Med Biol 2014;40(11):2707–14.
[26] Hansen PM, Pedersen MM, Hansen KL, Nielsen MB, Jensen JA. Examples of vector velocity imaging. IFMBE Proceedings: Springer; 2011. p. 77–80.
[27] Pedrizzetti G, La Canna G, Alfieri O, Tonti G. The vortex – an early predictor of cardiovascular outcome? Nat Rev Variol 2014;11:545–53.